



# Room Temperature Synthesis of Nanostructured ZnO: Active Visible Photocatalyst in the Degradation of Methylene Blue

**Amine El Farrouji<sup>1,2\*</sup>, Rachid Mohamed Tchalala<sup>2</sup>, Abderrahim Chihab Eddine<sup>1</sup>, Ahmad Mehdi<sup>3</sup>, Larbi El Firdoussi<sup>2</sup> and Mustapha Ait Ali<sup>2</sup>**

<sup>1</sup>*Laboratoire de Chimie Appliquée et Environnement, Faculté des Sciences Ibn Zohr, Agadir, Morocco.*

<sup>2</sup>*Laboratoire de Chimie de Coordination et Catalyse, Faculté des Sciences Semlalia, Marrakech, Morocco.*

<sup>3</sup>*Laboratoire de Chimie Moléculaire et Organisation du Solide, Université Montpellier, Montpellier, France.*

## **Authors' contributions**

*This work was carried out in collaboration among all authors. All authors read and approved the final manuscript.*

## **Article Information**

DOI: 10.9734/CSJI/2021/v30i330220

### Editor(s):

(1) Dr. P. Thomas. West, Texas A&M University-Commerce, USA.

### Reviewers:

(1) Senthil Kumar, National Institute of Technology, India.

(2) Yimer, Wondwossen Melaku, Mizan - Tepi University, Ethiopia.

Complete Peer review History: <http://www.sdiarticle4.com/review-history/68268>

**Original Research Article**

**Received 01 March 2021**

**Accepted 07 May 2021**

**Published 11 May 2021**

## **ABSTRACT**

Nanostructured ZnO was prepared using a facile solution-phase method at room temperature without need to calcination. Oxidation of zinc sulfate by sodium hypochlorite in the presence of polyethylene glycol (PEG) and sodium hydroxide (NaOH) gave pure nanostructured zinc oxide (ZnO-NPs). The structure and physicochemical properties of the material were determined by X-ray powder diffraction (XRD), Fourier-transform infrared spectroscopy (IR), Energy Dispersive X-ray Spectroscopy (EDS), Scanning Electron Microscopy (SEM), Transmission Electron Microscopy (TEM), UV-Vis diffuse reflectance and their optical Properties. ZnO particles were successfully distributed in two-dimensional sheet with a nanometric thickness and a random distribution. The activity was evaluated for photocatalytic degradation of methylene blue (MB) by a study of experimental conditions such as the effect of the mass of the catalyst, the effect of the initial concentration of the dye and the effect of the volume of the oxidizing agent. The kinetics of the reaction follow a pseudo-first order.

\*Corresponding author: E-mail: a.elfarrouji@gmail.com;

**Keywords:** Nanostructured ZnO; Nanosheets; band-gap, photocatysis, methylene blue.

## 1. INTRODUCTION

Recently, a wide range of research on synthesizing metal oxides have gained much importance due to their potential applications in various fields [1]. Among these metal oxides, zinc oxide attracted the scientists as it is low cost, environmentally benign and efficient semiconductor. Zinc oxide is a commercially important material used in solar cells [2], rubber [3], sensors [4], varistors [5], etc. and exhibiting many significant properties such as piezoelectricity [6], catalysis [7] and novel optical properties [8].

Because of its interesting properties, zinc oxide has been prepared using a variety of methods such as solvothermal process [9], sonochemical method [10], thermal evaporation method [11], laser ablation [12], chemical vapor deposition [13], sol-gel [14], microwave-assisted strategies [15]. These routes always require high temperature, complex apparatus or other rigid conditions. In addition, methods that work in the laboratory cannot always be applied on an industrial scale, where it is important for the process to be economically effective, high yielding and simple to implement. Since precipitation approach compared with other traditional methods provides a facile way for low cost and large-scale production, which does not need expensive raw materials and complicated equipment's, so they have been proved to be promising ways to synthesize ZnO nanostructure.

Nowadays, environmental pollution has become one of the most severe challenges. Organic dyes are compounds widely used in textile, paper, plastic and cosmetic industries and are easily recognized as pollutants. Methylene Blue (MB) is typical dye in the textile industry which appear resistant to biodegradation [16]. Most conventional methods for the removal of dye pollutants such as adsorption on activated carbon [17], ultrafiltration [18], reverse osmosis [19], etc. are non-destructive and merely transfer pollutants from one phase (for example, aqueous) to the other (for example, adsorbent). The photocatalysis has shown a great potential and is extensively employed, because of its capacity to degrade recalcitrant chemicals in both gaseous and aqueous systems. The literature is abundant in reports mentioned that ZnO nanoparticles can be used to degrade organic contaminants and to convert them into

benign materials safe for the environment and humans [20]. Nanoscale ZnO exhibits high photocatalytic activity because of its numerous active sites and significant surface area [21].

Herein, we report the synthesis of nanostructured ZnO using a fast, facile and inexpensive solution method which should be suitable for large-scale production. The synthesis was realized at room temperature from commercially available Zinc sulfate in the presence of sodium hydroxide, aqueous solution of sodium hypochlorite (12% NaOCl) and polyethylene glycol (PEG) as surfactant agent. Catalytic activity of nanostructured ZnO was investigated in the photocatalytic oxidation of methylene blue (MB) under visible light in the presence of sodium hypochlorite.

## 2. METHODOLOGY

### 2.1 Synthesis of Nanostructured ZnO

All reagents were analytical grade and used without further purification. The precursor solution was prepared by dissolving 1 g of zinc sulfate heptahydrate powder in 50 mL of distilled water. Then, 0.2 g of polyethyleneglycol (PEG) was added under continuous stirring. The resulting mixture was stirred at room temperature for an additional 10 min until a clear and homogeneous solution was obtained. Subsequently, 20 mL of sodium hypochlorite (12%) was added and 0.3M of aqueous NaOH was added drop-wise to the obtained solution under vigorous stirring to yield a white milky precipitate. Vigorous stirring was maintained for an additional 30 min period at room temperature. The resulting precipitate was filtered, washed with distilled water several times and dried either at room temperature or at 80°C. The phase structure was examined by XRD Diffractometer (Bruker D8 Discover) using a Cu K $\alpha$  radiation (0.1541nm). The morphology of the products was investigated by a scanning electron microscope (SEM, Jeol JMSM5500), MET (JEOL 2200 FS) and EDS spectrum. Optical proprieties also the photoluminescence (PL) emission spectra were taken on a PANalytical AXIOS Max spectrophotometer.

### 2.2 Photocatalytic Oxidation of Methylene Blue

To 50 mL of Methylene Blue ([BM] = 10mg/L) solution was added 10mg of ZnO nanoparticle.

The mixture was stirred for 15min to have thermodynamic equilibrium and good dispersion of the catalyst. 10 ml of NaOCl (12%) were added and the mixture was then illuminated with an ordinary tungsten lamp (visible light). The mixture was left stirring at room temperature and measuring the absorbance performed in separate time intervals.

### 3. RESULTS AND DISCUSSION

#### 3.1 Structural Proprieties of the Synthesized ZnO Nanomaterials

The general morphologies of as-synthesized ZnO-NPs was analyzed by scanning electron microscopy (SEM) which reveals two-dimensional sheet with a nanometric thickness and a random distribution (Fig. 1(a) and (b)).

The crystallinity of the synthesized ZnO-NPs was examined by X-ray diffraction (Fig. 2). Several well-defined diffraction reflections were appeared in the pattern 31.6, 34.3, 36.2, 47.5, 56.6, 62.8, 68.1, 69.3 and 78.2 which correspond to the lattice planes of (110), (002), (101), (102), (110), (103), (112), (201) and (202), respectively. ZnO crystallize in wurtzite structure, hexagonal phase ( $a = 0.3351$  nm,  $c = 0.5226$  nm) with the space group  $P6_3mc$ .

Diffraction peaks related to the impurities were not observed in the XRD pattern, confirming the high purity of the synthesized product. Furthermore, it could be seen that the diffraction peaks were more intensive and narrower, implying a good crystallinity (JCPDS data card n°: 36-1451).

The average crystallite sizes were estimated according Debye - Scherrer formula. whose average size calculated from directions (100), (002) and (101) is of the order of 31,39 nm (Table 1).

This fact was further confirmed by energy dispersive spectroscopy (EDS). As can be seen from the observed EDS spectrum, only zinc and oxygen peaks are very clear and important, with only one insignificant peak related to impurities, which again confirmed the high purity of ZnO-NPs (Fig. 3).

The prepared ZnO-NPs was analyzed by Fourier transform infrared (FTIR) spectroscopy (Fig. 4).

Several well-defined bands at 540, 1630 and 3460  $\text{cm}^{-1}$  are detected in the FTIR spectrum. The origination of a well-defined band at 540 $\text{cm}^{-1}$  is due to Zn-O modes and hence confirms the formation of ZnO.

Fig. 5 shows the TEM images of the ZnO-NPs before and after recycling. It can be seen that the morphology remains almost the same, which justifies the possibility of reusing the ZnO-NPs for several cycles.

**Table 1. Average crystallite sizes estimated according Debye - Scherrer formula**

hkl	2θ (deg)	FWHM (deg)	D (nm)
100	31,6	0,2598	31.8
002	34.3	0,2273	36.6
101	36,2	0,3247	25.77

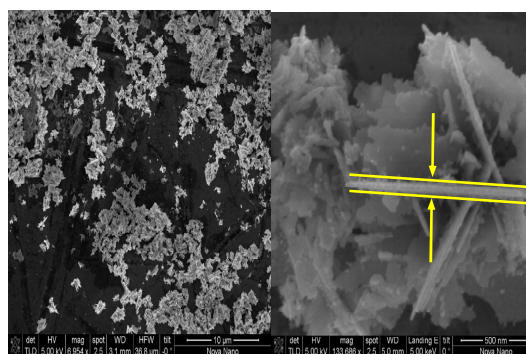


**Fig. 1. SEM images of synthesized ZnO-NPs**

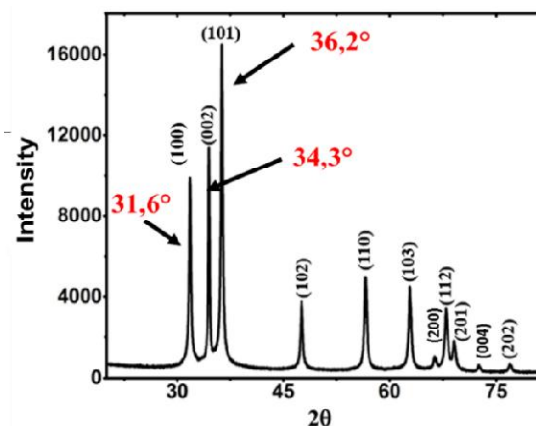


**Fig. 2. XRD patterns of synthesized ZnO-NPs**

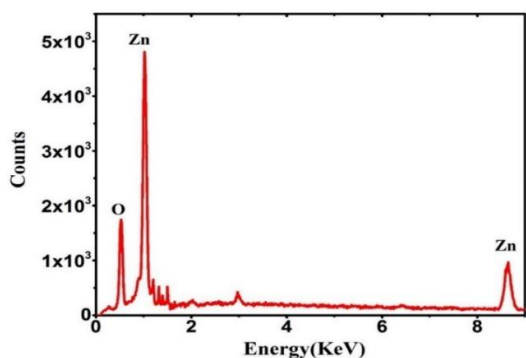


Fig. 3. EDS Spectrum of synthesized ZnO-NPs

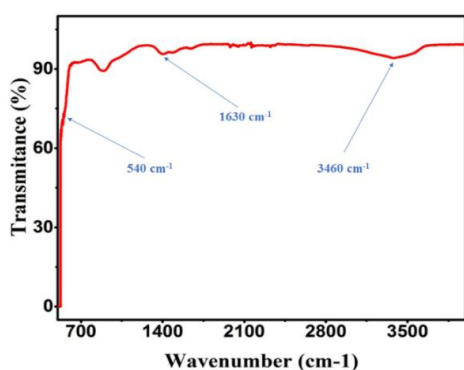


Fig. 4. FTIR spectrum of synthesized ZnO-NPs

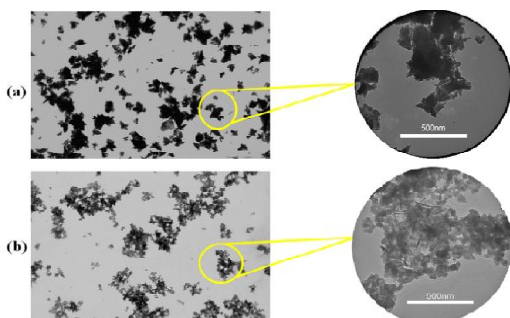


Fig. 5. TEM images: (a) before recycling; (b) after recycling

### 3.2 Optical Properties of Synthesized ZnO

The UV-Vis spectra of the samples are shown in Fig. 6. The absorption edge of the ZnO was observed at 397nm. The optical band gap energy was estimated to be about 3.12 eV from the absorption onset measured by the extrapolation of the linear portion of the graph between modified Kubelka-Munk function  $[F(R) / h\nu]^2$  versus photon energy ( $h\nu$ ). ZnO exhibits also a

sharp band at 368 nm, which correspond to the formation of nanoparticles [22].

The photoluminescence (PL) characteristics of the synthesized ZnO nanoparticles were obtained at room temperature in the wavelength range 300-600 nm. In the spectrum (Fig. 7) two luminescence bands are observed; a short and weak wavelength band centered at around 392nm, and a broad, strong and dominated band located at long-wavelength in the 520nm. The assignment of this band in ZnO is generally poorly understood in all forms of the sample. The UV emission band is due to near band-edge transition, and the broad emission originates from the recombination of a photogenerated hole with the single ionized charge state of the single ionized oxygen vacancy. Notably, the observation of such strong emission band from excitons rather than from defects implies that the as obtained ZnO nanocrystals bear high crystallinity or low lattice disorder [23-24].

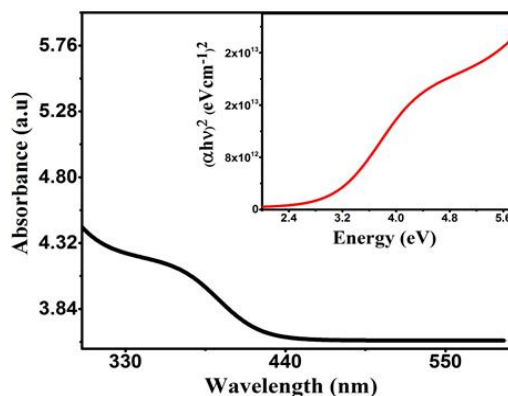


Fig. 6. UV-Vis absorption spectrum and band gap estimation of ZnO nanoparticles

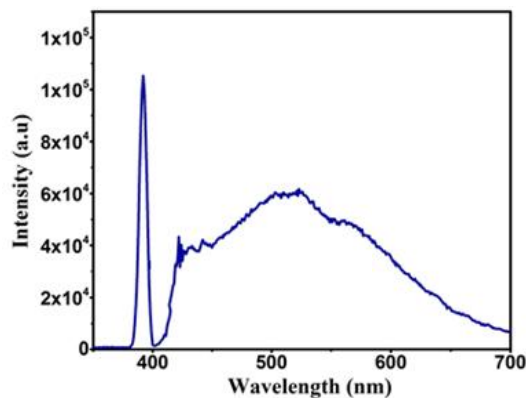


Fig. 7. PL spectra of the as-synthesized ZnO nanoparticles

### 3.3 Catalytic Activity of Nanostructured ZnO

To explore the potential capability of the obtained ZnO-NPs to remove contaminants from wastewater, the catalytic activity was evaluated in the photodegradation of MB in the presence of NaOCl. Experiments were carried out both in the presence and in the absence of catalyst. In the absence of NaOCl, no considerable photodegradation of MB took place after 60 min. Without the use of visible light, the reaction with ZnO-NPs/NaOCl is not complete even after 180 minutes stirring and reaches only 59.18% (Fig. 8a).

Under visible light, total discoloration of the reaction mixture was observed after 40 min in the presence of ZnO/NaOCl system. UV-Visible spectra (Fig. 8b), shows the reduction in the  $\lambda_{max}$  of Methylene Blue over time.

After 40min, 98% of MB removal was occurred. In addition, the shift of the absorbance maximum to shorter wavelengths (hypsochromic effect) is not observed, which shows that N-demethylation of MB auxochromic groups does not take place during the catalytic oxidation. A similar effect was observed by other authors studying the photocatalytic oxidation of MB [25].

#### 3.3.1 Initial conditions of MB degradation study

A series of degradation reaction were carried out with different mass of ZnO (from 5mg to 20mg) using 50mL solution of varied BM concentration

(from 10mg / L to 30mg/L) and different volume of NaOCl 12% (from 5mL to 20mL) (Table 2).

It is noted that the catalytic activity increases with the increase of the initial ZnO mass up to a critical mass of 10 mg, beyond which the percentage of the degradation decreases (*entry 1, 2, 3 and 4*). The effect of the initial BM concentration on catalytic activity was studied using different starting concentration for BM (*entry 1, 5 and 6*) for a duration of 40 min. The degradation decreases slightly with the initial concentration of BM. For a solution of 50mL of BM (10mg / L) and optimal mass (10mg) of ZnO, increasing the volume of NaOCl 12% (*entry 1, 7, 8 and 9*), the catalytic activity also increases.

#### 3.3.2 Kinetic study

For the evaluation of the reaction rate, a kinetic study has been carried out which shows that the reaction is pseudo-first order verified by monitoring the evolution of the BM absorbance at different times. The graph in Fig. 9 shows the variation of  $\ln(C_0/C_t)$  as a function of time. The line obtained  $\ln(C_0/C_t) = kt$  with a  $R^2 = 0.96$ , confirms that the reaction is pseudo-first order so the constant of the velocity  $k = 0.0648 \text{ min}^{-1}$  is obtained from the slope.

#### 3.3.3 Recycling of ZnO-NPs catalyst

For further evaluation of the catalytic efficiency of ZnO, a recycling study was conducted. For that after 40min of the reaction, ZnO-NPs is recovered by centrifugation and reused several times. From Table 3 it can be seen that ZnO catalyst can be used up to three times with a slight decrease in catalytic activity.

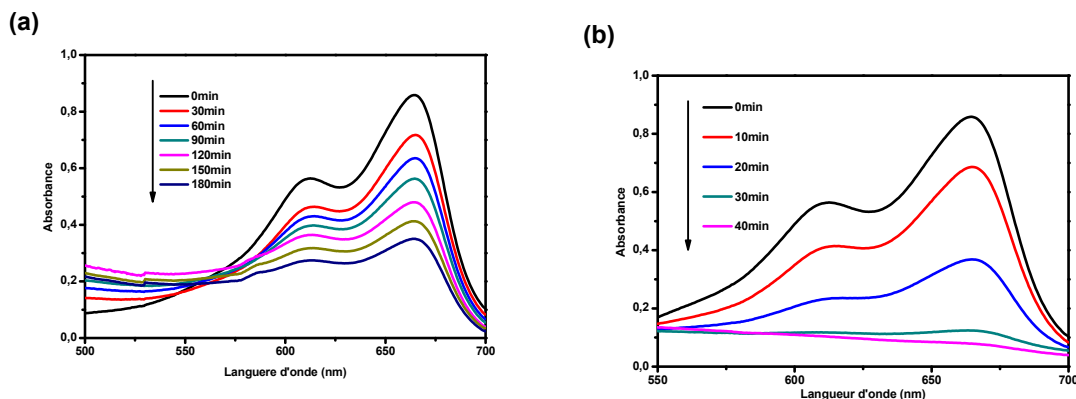


Fig. 8. UV-visible spectra obtained during the MB degradation in the presence of ZnONst/NaOCl: (a) without light (b) under visible light

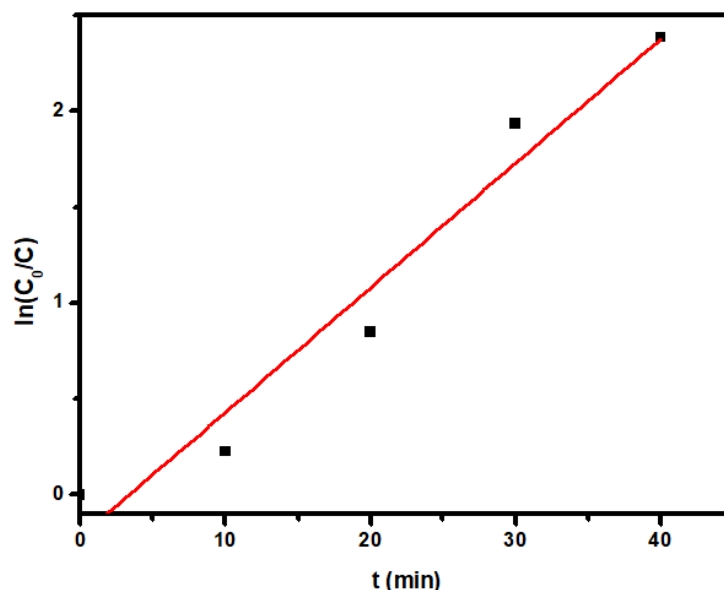
Fig. 9.  $\ln(C_0/C)$  as a function of time

Table 2. study of initials conditions of MB degradation

Entry	Mass of ZnO (mg)	Concentration of MB (mg/L)	Volume of NaOCl (mL)	% Degradation
1	5	10	10	74
2	10	10	10	<b>98</b>
3	15	10	10	97
4	20	10	10	90
5	10	20	10	90
6	10	30	10	88
7	10	10	5	84
8	10	10	15	96
9	10	10	20	95

*time: 40min, room temperature*

Table 3. recycling of ZnO-NPs

N° of cycle	% degradation
1	<b>98</b>
2	95.12
3	90.25

*time: 40min; [MB] = 10mg/L; m(ZnO) = 10mg; V(NaOCl) = 10mL*

#### 4. CONCLUSION

We have succeeded in producing hierarchical structures of ZnO nanosheets by a solution route at ambient conditions (room temperature and atmospheric pressure). PEG play an important role in the formation ZnO hierarchal nanosheet structures. Efforts are now geared towards making non- agglomerated sheets. The use of

ZnO nanostructures shows its effectiveness for degradation of methylene blue using NaOCl (12%) as an oxidizing agent. This efficiency has been increased using visible light irradiation.

#### COMPETING INTERESTS

Authors have declared that no competing interests exist.



## REFERENCES

1. Athar T. Emerging Nanotechnologies for Manufacturing, Second Edition. Chapter 14, 2015;343–401.
2. Z Chamanzadeha V, Ansarib M Zahedifar. Investigation on the properties of La-doped and Dy-doped ZnO nanorods and their enhanced photovoltaic performance of Dye-Sensitized Solar Cells. *Optical Materials*. 2021;112:110735. Available:<https://doi.org/10.1016/j.optmat.2020.110735>
3. Yong Hwan Lee, Misuk Cho, Jae-Do Nam, Youngkwan Le. Effect of ZnO particle sizes on thermal aging behavior of natural rubber vulcanizates. *Polymer Degradation and Stability*. 2018;148:50-55. Available:<https://doi.org/10.1016/j.polyimdegradstab.2018.01.004>
4. Ping-Che Lee, Yu-Liang Hsiao, Dutta Jit, Ruey-Chi Wang, Shih-Wen Tseng, Chuan-Pu Liu. Development of porous ZnO thin films for enhancing piezoelectric nanogenerators and force sensors. *Nano Energy*. 2021;82:105702. Available:<https://doi.org/10.1016/j.nanoen.2020.105702>
5. Wenfeng Liu, Lei Zhang, Fanyi Kong, Kangning Wu, Shengtao Li, Jianying Li. Enhanced voltage gradient and energy absorption capability in ZnO varistor ceramics by using nano-sized ZnO powders. *Journal of Alloys and Compounds*. 2020;828:154252. Available:<https://doi.org/10.1016/j.jallcom.2020.154252>
6. Xiaoting Zhang, Minh-Quyen Le, Omar Zahhaf, Jean-Fabien Capsal, Pierre-Jean Cottinet, Lionel Petit. Enhancing dielectric and piezoelectric properties of micro-ZnO/PDMS composite-based dielectrophoresis. *Materials & Design*. 2020;192:108783. Available:<https://doi.org/10.1016/j.matdes.2020.108783>
7. Amr Fouda, Salem S Salem, Ahmed R Wassel, Mohammed F Hamza, Th I Shaheen. Optimization of green biosynthesized visible light active CuO/ZnO nano-photocatalysts for the degradation of organic methylene blue dye. *Heliyon*. 2020;6(9):e04896. Available:<https://doi.org/10.1016/j.heliyon.2020.e04896>
8. Ahmad A Ahmad, Qais M Al-Bataineh, Ahmad M Alsaad, Tariq O Samara, Kholoud A Al-izy. Optical properties of hydrophobic ZnO nano-structure based on antireflective coatings of ZnO/TiO<sub>2</sub>/SiO<sub>2</sub> thin films. *Physica B: Condensed Matter*. 2020;593:412263, Available:<https://doi.org/10.1016/j.physb.2020.412263>
9. Xu Zhang, Jianping Chen, Mengyang Wen, Haibo Pan, Shuifa Shen. Solvothermal preparation of spindle hierarchical ZnO and its photocatalytic and gas sensing properties. *Physica B: Condensed Matter*. 2020;412545. Available:<https://doi.org/10.1016/j.physb.2020.412545>
10. Yan Bao, Lu Gao, Caiping Feng, Jianzhong Ma, Wenbo Zhang, Chao Liu, Demetra Simion. Sonochemical synthesis of flower-like ZnO assembled by hollow cones toward water vapor permeability and water resistance enhancement of waterborne film. *Journal of Industrial and Engineering Chemistry*. 2020;82:180-189. Available:<https://doi.org/10.1016/j.jiec.2019.10.011>
11. Azmi FFA, Kadir MFZ, Shujahadeen B Aziz, Muzakir SK. Characterization of optoelectronic properties of thermally evaporated ZnO. *Materials Today: Proceedings*. 2020;29(1):179-184. Available:<https://doi.org/10.1016/j.matpr.2020.05.539>
12. Ayman M Mostafa, Eman A Mwafy. Synthesis of ZnO and Au@ZnO core/shell nano-catalysts by pulsed laser ablation in different liquid media. *Journal of Materials Research and Technology*. 2020; 9(3):3241-3248. Available:<https://doi.org/10.1016/j.jmrt.2020.01.071>
13. Swathia S, Sunil Babub E, Yuvakkumar R, Ravi G, Arunachalam Chinnathambi, Sulaiman Ali Alharbi, Dhayalan Velauthapillaid. Branched and unbranched ZnO nanorods grown via chemical vapor deposition for photoelectrochemical water-splitting applications. *Ceramics International*;2020.Available:<https://doi.org/10.1016/j.ceramint.2020.12.119>
14. Perveen R, Shujaat S, Qureshi Z, Nawaz S, Khan MI, Iqbal M. Green versus sol-gel synthesis of ZnO nanoparticles and antimicrobial activity evaluation against panel of pathogens. *Journal of Materials*

- Research and Technology. 2020;9(4):7817-7827.  
Available: <https://doi.org/10.1016/j.jmrt.2020.05.004>
15. Radhakrishnan JK, Kumara Geetika M. Growth of ZnO nanostructures: Cones, rods and hollow-rods, by microwave assisted wet chemical growth and their characterization. *Ceramics International*; 2020.  
Available: <https://doi.org/10.1016/j.ceramint.2020.10.110>
  16. Ghanizadeh Gh, Asgari G. Adsorption kinetics and isotherm of methylene blue and its removal from aqueous solution using bone charcoal. *React. Kinet. Mech. Catal.* 2011;102:127–142.
  17. Lindong Li, Mingbang Wu, Chuhan Song, Lin Liu, Wenli Gong, Yanhong Ding, Juming Yao. Efficient removal of cationic dyes via activated carbon with ultrahigh specific surface derived from vinasse wastes. *Bioresource Technology*. 2021; 322:124540.  
Available: <https://doi.org/10.1016/j.biortech.2020.124540>
  18. Said Benkhaya, Souad M'rabet, Rachid Hsissou, Ahmed ElHarfi. Synthesis of new low-cost organic ultrafiltration membrane made from Polysulfone/ Polyetherimide blends and its application for soluble azoic dyes removal. *Journal of Materials Research and Technology*. 2020;9(3): 4763-4772.  
Available: <https://doi.org/10.1016/j.jmrt.2020.02.102>
  19. Trishitman Das, Alfredo Cassano, Angelo Basile, Navin K Rastogia. Reverse osmosis for industrial wastewater treatment. *Current Trends and Future Developments on (Bio-) Membranes. Reverse and Forward Osmosis: Principles, Applications, Advances* 2020;207-228.  
Available: <https://doi.org/10.1016/B978-0-12-816777-9.00009-5>
  20. Khan Idrees, Saeed Khalid, Ali Nisa, Khan Ibrahim, Zhang Baoliang, Sadiq Muhammad. Heterogeneous photo-degradation of industrial dyes: An insight to different mechanisms and rate affecting parameters. *Journal of Environmental Chemical Engineering*. 2020;8(5):104364.  
Available: <https://doi.org/10.1016/j.jece.2020.104364>
  21. Getu Kassegn Weldegebrieal. Synthesis method, antibacterial and photocatalytic activity of ZnO nanoparticles for azo dyes in wastewater treatment: A review. *Inorganic Chemistry Communications*. 2020;120:108140.  
Available: <https://doi.org/10.1016/j.inoche.2020.108140>
  22. Janotti A, VandeWalle CG. Fundamentals of zinc oxide as a semiconductor. *Rep. Prog. Phys.* 2009;72:126501–126529
  23. Huang MH, Wu Y, Feick H, Tran N, Weber E, Yang P. Catalytic growth of zinc oxide nanowires by vapor transport. *Advanced Materials*. 2001;13(2):113–116.
  24. Williams G, Kamat PV. Graphene-semiconductor nanocomposites: Excited-state interactions between ZnO nanoparticles and graphene oxide. *Langmuir*. 2009;25(24):13869–13873.
  25. Zhang T, Oyama T, Aoshima A, Hidaka H, Zhao J, Serpone N. Photooxidative N-demethylation of methylene blue in aqueous TiO<sub>2</sub> dispersions under UV irradiation. *J Photochem. Photobiol. A: Chem.* 2001;140(2):163-72.

© 2021 El Farrouji et al.; This is an Open Access article distributed under the terms of the Creative Commons Attribution License (<http://creativecommons.org/licenses/by/4.0>), which permits unrestricted use, distribution, and reproduction in any medium, provided the original work is properly cited.

*Peer-review history:*

*The peer review history for this paper can be accessed here:*  
<http://www.sdiarticle4.com/review-history/68268>